Electronic Journal of Structural Engineering

Original Article

Cite this: DOI:10.56748/ejse.24766

Received Date: 1 March 2024
Accepted Date: 15 July 2025

1443-9255
https://ejsei.com/ejse


# Heat and abrasion resistance of fly ash geopolymer mortar comprising ceramic polishing waste and cured with different conditions

**Jay Kiritkumar Bhavsar [a*], Vijay Ramanlal Panchal [a]**

[a] M. S. Patel Department of Civil Engineering, Chandubhai S. Patel Institute of Technology, Faculty of Technology & Engineering, Charotar University of Science and Technology, Changa, Anand, Gujarat 388421, India.
*Corresponding author: jaybhavsar.cv@charusat.ac.in

## Abstract

The rising demand for geopolymer concrete (GPC) is associated with its lower environmental impact. GPC has significant potential for the use of industrial by-products as a geopolymer precursor. The vitrified and wall tile polishing processes produce two types of ceramic polishing waste (CPWs): vitrified tile CPW (VCPW) and wall tile CPW (WCPW). In this study, fly ash (FA), CPW, and alkaline activators were used to make geopolymer mortar (GM). This study investigates the heat and abrasion resistance of GM cured under three curing conditions (ambient, 60°C for 24 hours, and 60°C for 48 hours). The microstructure after heat exposure was analyzed by scanning electron microscopy (SEM). In addition, the GM samples were tested for surface abrasion and compressive strength. The outcomes revealed that replacing FA with 15% CPWs improves early-age compressive strength and abrasion resistance and provided similar performance in heat resistance at 1000°C. The curing conditions strongly influenced early-age compressive strength and fire exposure performance at 500°C. The microstructure of the geopolymer shows additional geopolymerization due to heat exposure and reduced degradation of the gel. Replacing FA with 15% VCPW or WCPW enhances the heat and abrasion resistance of GM.

## Keywords

**Fire resistance, Abrasion wear, Ceramic polishing waste, Microstructure, Ambient curing, Temperature curing**

## 1. Introduction

Concrete is a widely consumed material, next to water. The production of concrete substantially exacerbates greenhouse gas emissions and also demands extensive natural resources (Chindaprasirt et al., 2010; Belaïd, 2022). The consumption of cement for concrete and other construction materials has been increasing. Moreover, the significant amount of $CO_2$ emissions associated with cement production can hinder sustainable development. To address these issues, researchers are working to reduce cement usage by partially replacing it with supplementary cementitious materials (SCMs). (Zareei et al., 2017; Phul et al., 2019; Al-Hashem et al., 2022; Runganga, Okonta and Musonda, 2024). Conversely, geopolymer binders have demonstrated enhanced environmental sustainability. Industrial byproducts such as fly ash (FA), ground granulated blast furnace slag (GGBS), rice husk ash (RHA), and ceramic waste are used as precursors (Saranya, Nagarajan and Shashikala, 2019; Bhavsar and Panchal, 2022; Memiş and Bılal, 2022). FA geopolymer binder is a superior option to traditional concrete as it gives sufficient strength, economy, durability, and a low $CO_2$ footprint (Singh, 2018). The GPC is durable against heat, chloride, acid, and wear (Wong, 2022). Industrial waste, which is abundant in silicon dioxide and aluminum oxide, can be combined with an alkaline solution to produce geopolymer.

Ceramic building materials are in tremendous demand in several emerging nations. Ceramic polishing wastes (CPWs) are a byproduct formed during the polishing and glazing operations. Improper disposal of these wastes leads to pollution of land, water, and air. (Raval, Patel and Pitroda, 2013; Patel, Arora and Vaniya, 2015). Environmental scientists are primarily interested in methods to reuse this kind of waste. The literature reported the use of CPW as a cement replacement. The optimal percentage of such replacement was in the range of 10-20% (El-Dieb et al., 2018). In a similar kind of study, authors examined the OPC mortar prepared with ceramic waste (CW) and micro-silica (MS). The compressive strength (CS) increases with 15% of CW and 10% of MS but decreases with further addition. The water absorption and sorptivity decreased, with 15% of CW, and the expansion remains lower (Nayana and Rakesh, 2018). The ceramic fines (CF) as a part substitution for FA were utilized for making geopolymer mortar (GM). The outcome showed a positive impact with increasing temperatures and replacing 25% of CF with FA. Microstructure analysis revealed that an increase in CF increased porosity (Kalinowska-Wichrowska et al., 2024). The use of CW as ground granulated blast furnace slag (GGBS) replacement showed a promising application as a geopolymer binder (Aly et al., 2018). The use of red CW as a metakaolin replacement for GM improved the particle packing. Up to 33% replacement of CW did not reduce the strength of GM (Krishna Rao and Kumar, 2020). Researchers looked at how different amounts of NaOH and $Na_2SiO_3$ affected the mechanical properties of a GM made from ceramic powder. Researchers found that the CS of GM ranged from 10.5 MPa to 41.5 MPa. The 15% Na and 0 silica modulus, and 0.4 water to powder ratio gave the highest compressive and flexural strength (M Kaya, 2022). The use of 5% of CW as FA replacement cannot affect the mechanical and durability properties of temperature-cured GPC. Increasing the replacement of CW in place of FA reduces the $CO_2$ emissions of GPC (Saxena and Gupta, 2022). The use of broken ceramic tile waste as a fine aggregate replacement for FA-based GM improved the CS (Yanti et al., 2024). In the past, different ceramic crushed powders were used for making FA geopolymer. Such powders can be obtained by crushing bricks, floor tiles, and sanitary waste. The study suggested that the types of ceramic powder and their optimum percentage are critical factors for creating efficient GM (Herbudiman et al., 2024). In another study, a fire test was performed at 900°C for alkali-activated mortar made with GGBS and replaced by CW and FA. The replacement of FA by GGBS reduced the CS, but GM with 50% of CW, 20% of GGBS, and 10% of FA performed best (Huseien et al., 2018). The alkali-activated paste made from CW and GGBS was tested at 200°C to 1000°C for 2 hours (h). The increase in CW in paste gave improved resistance to high temperatures (Rashad and Essa, 2020). The effect of extreme heat on geopolymer paste made from CW, FA, and GGBS was studied in the past. The waste ceramic powder enhanced the mechanical strength, reduced cracks, and improved the microstructure after heat exposure (Zhang et al., 2021).

CW and RHA were used in place of GGBS to create GPC, which is more heat resistant than conventional concrete. The CW-based GPC exhibited superior heat resistance in comparison to RHA-based GPC (Memiş and Bılal, 2022). Degirmenci (2018) tested GM at high temperatures and freeze-thaw cycles with FA, slag, and natural zeolite (NZ) as base materials. The freeze and thaw test significantly impacts the weight loss of NZ-based GM, surpassing that of GGBS- and FA-based GM. The residual CS (RCS) of NZ-based mortars is higher than that of FA and GGBS-based mortars. Hager et al. (2021) examined the impact of heat (1000 °C) on FA-based GM. They used FA as the primary binder and varied the content of slag replacement. The slag addition improves GM's mechanical performance, but GM without slag performs better at high temperatures (Hager, Sitarz and Mróz, 2021).

Ahmed et al. (2024) designed geopolymer composites that incorporated GGBS, brick waste powder (BWP), and FA. They cured the samples in an oven. Flexural strength and abrasion resistance decreased as BWP increased. However, water absorption and sorptivity increased when BWP increased (Ahmed, Atmaca and Khoshnaw, 2024). GPC has a

lower abrasion value than conventional concrete (Ramujee and Potharaju, 2014). The wear and heat resistance of GM made with GGBS are higher than those of cement mortar (Bingöl et al., 2020). Witzke et al. (2023) tested metakaolin-based GPC containing 10% RHA for abrasion. The abrasion resistance of GPC was similar or superior to that of ordinary concrete (Witzke et al., 2023). One-part GPC slabs experience higher abrasion compared to traditional concrete. The increasing slag content and higher water levels lead to greater abrasion. The performance of GPC depends on microstructural behavior and microstructural properties (Negahban, Bagheri and Sanjayan, 2023). Vilas Meena et al. (2022) tested self-compacting concrete for fire and abrasion resistance. The ceramic waste tile aggregates enhanced the performance against fire and abrasion (Vilas Meena et al., 2022). Geopolymer materials utilized in construction must have fire resistance capacity that fulfills the necessary duration requirements, taking into sustainability concerns (Hassan et al., 2023).

The literature encapsulates the investigation of the fire and abrasion resistance of GM, paste, and concrete. In the majority of investigations, ceramic broken tile powder served as an auxiliary binder, frequently substituting GGBS, which is a calcium-rich alkali-activated binder. The abrasion and fire resistance of GM produced with ceramic polishing waste as a replacement for FA was not documented to the best of our knowledge. Also, the energy required to transform CPW into powder is less compared to crushed ceramic tile waste. The substitution of FA with CPW constitutes a low calcium geopolymer binder which is different than higher slag-based GM. Further, earlier research did not highlight how abrasion and fire affected CPW-based GM that was cured in different conditions over time, such as ambient temperature, in an oven at 60°C for 24 and 48 hours. In this study, the high molarity (14 M) of NAOH and optimum ratio of $Na_2SiO_3$ to NaOH (2.5) were adopted, which is different from the previous study. Such alkaline mix criteria helped in achieving high CS at ambient temperature. The temperature curing processes considerably affect the low-calcium FA GM; therefore, the temperature regime is emphasized here. The study focused on efficient curing methods to improve the heat and abrasion resistance of GM. The present study replaced FA with 15% of CPWs, referencing previous research (Bhavsar and Panchal, 2022). However, it restricts successive replacements as it diminishes the compressive strength of GM.

## 2. Materials and Methods

CPW in sludge form was obtained from the ceramic tile industry and subsequently processed in the laboratory. The ceramic sludge was dried in an oven to eliminate moisture, and then it was crushed in a ball mill to get a fine powder (Fig. 1). The treated CPWs, specifically vitrified tile CPW (VCPW) and wall tile CPW (WCPW), were evaluated for their key properties (Table 1 and Table 2).

***Table 1. Chemical properties of precursors (% mass)***

| Metal Oxide | FA | VCPW | WCPW |
|---|---|---|---|
| $SiO_2$ | 58.98 | 70.71 | 57.55 |
| $Al_2O_3$ | 15.19 | 11.56 | 11.55 |
| $Fe_2O_3$ | 12.58 | 2.86 | 7.77 |
| CaO | 01.82 | 3.45 | 10.86 |
| Mg | 00.62 | 1.21 | 01.68 |
| $Na_2O$ | 00.25 | 1.39 | 00.96 |
| $K_2O$ | 01.88 | 3.39 | 01.50 |
| $SO_3$ | 01.60 | 0.46 | 02.88 |
| $P_2O_5$ | 00.58 | 0.16 | 00.28 |
| $TiO_2$ | 03.98 | 1.48 | 02.45 |
| ZnO | 00.20 | 1.17 | 01.23 |
| LOI | 001.2 | 0.66 | 02.33 |

***Table 2. Physical properties***

| Properties | FA | VCPW | WCPW |
|---|---|---|---|
| Specific Gravity | 2.500 | 2.529 | 2.530 |
| Surface Area ($cm^2/g$) | 5538 | 4976 | 5578 |


***Fig. 1 Treatment of ceramic waste***

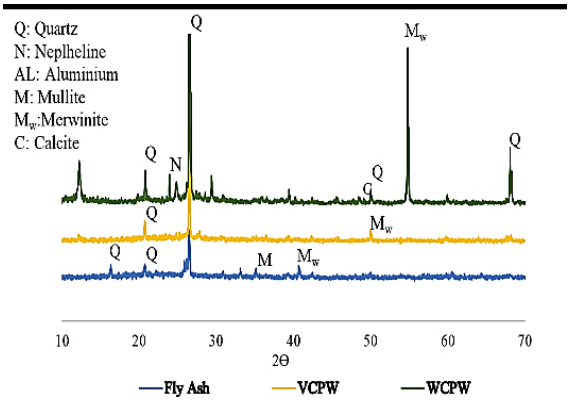


***Fig. 2 XRD of binders***

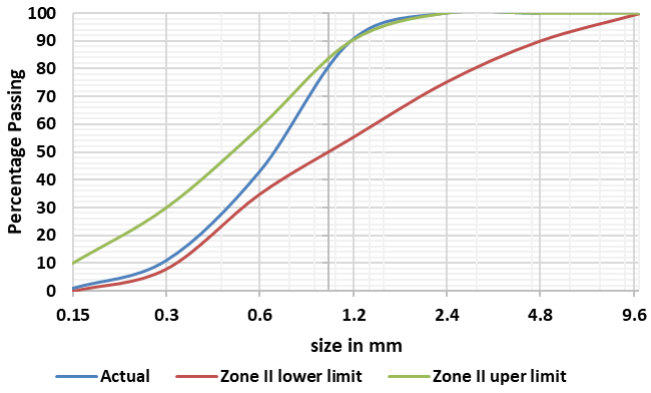


***Fig. 3 Grading curve for fine aggregates***

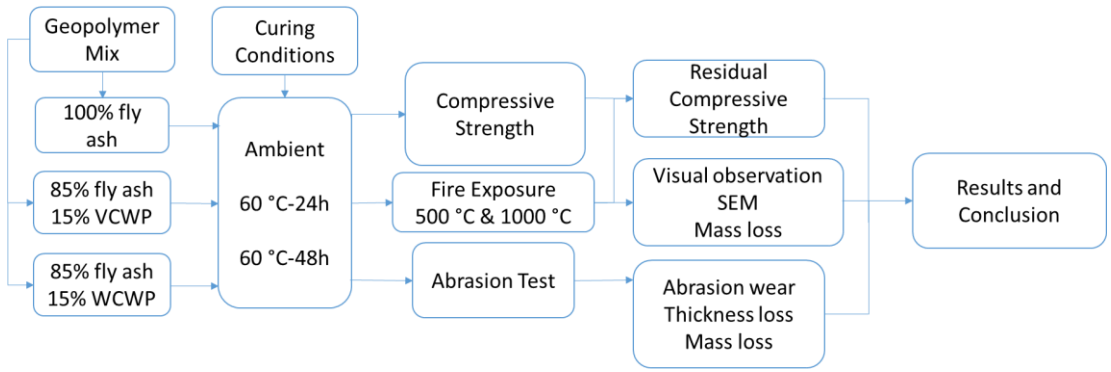


***Fig. 4 Research Methodology***

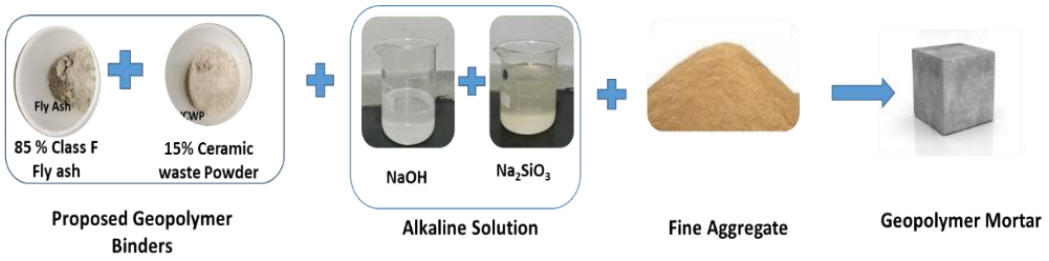


*Fig. 5 Making of Geopolymer Mortar*

*Table 3. Mix proportion of the GM (kg/m3)*

| Mix | FA | VCPW | WCPW | Fine aggregates | NS | NH | Curing regime |
|---|---|---|---|---|---|---|---|
| GPM | 730 | - | - | 1178 | 208.6 | 83.4 | 27°C - 30°C Ambient |
| GMV15 | 620 | 110 | - | 1178 | 208.6 | 83.4 | 60°C- 24 h oven |
| GMW15 | 620 | - | 110 | 1178 | 208.6 | 83.4 | 60°C - 48 h oven |

X-ray diffraction (XRD) was used to find the crystalline phases of CPWs (Fig. 2). The XRD pattern reveals an amorphous phase with a 2θ value ranging from 15°-30° for FA, 20°-30° for VCPW, and 23°-32° for WCPW.

The fine aggregates (sand) were classified in Zone II according to IS 383:2016 (Fig. 3). A 14 M NaOH (NH) solution was prepared with NaOH flakes of 97% purity. $Na_2SiO_3$ (NS) with a $SiO_2$ to $Na_2O$ molar ratio of 2.0 was procured in liquid form from a local vendor. $Na_2SiO_3$ contains 31.4% $SiO_2$, 15.9% $Na_2O$, and 52.7% $H_2O$, respectively.

Fig. 4 depicts the research method adopted for the study. The approaches focused on two goals: first, to recommend a new binder mixture, and second, to examine the impact of curing conditions on the strength and durability properties of GM.

The low-calcium binder requires thermal curing for geopolymerization. But, considering the advantages of in-situ casting and low energy use, ambient curing is the more feasible option.

Temperature curing adds tremendous value to precast applications and increases longevity due to its low permeability. As a result, ambient curing and two oven curing procedures were used in the study at 23°C–27°C and 60°C for 24 and 48 hours, respectively.

Fig. 5 illustrates the process of producing GM. The density of wet GM was taken as 2200 kg/m$^3$. The precursors comprised one-third of the entire mixture. The alkaline liquid-to-binder (A/B) proportion was 0.4, as previous research has shown that a 14M NH solution with a 0.4 A/B ratio produced the maximum CS (Krishna Rao and Kumar, 2020). The NS/NH ratio of 2.5 yields the maximum CS at all temperatures; hence, it is used (Joshi and Kadu, 2012).

The designed mixes are shown in Table 3. The NH solution was produced 24 hours before mixing. The NS and NH were combined prior to 30 minutes of wet mixing. For preparing for the GM, binders and fine aggregates were mixed manually under dry conditions. The alkaline liquids (NS and NH) were added to the dry mixture, and wet mixing was carried out for 5 to 6 minutes.

The GM was cast in a 70.6 mm cube mold. It was added in molds in two layers and subsequently compacted using a vibration machine for 30 seconds. The specimens intended for ambient curing were removed from the molds after 24 h and then kept at ambient temperature. Throughout the experiment, the ambient temperature ranged from 27°C to 30°C. The relative humidity ranged from 50 to 60 percent. The heat-curing samples were placed in the oven with the mold (Fig. 6) and heated at 60°C for 24 hours and 48 hours (Table 3). After the oven curing, samples were stored at room temperature for normal curing until testing. Each set of tests involved testing three specimens.

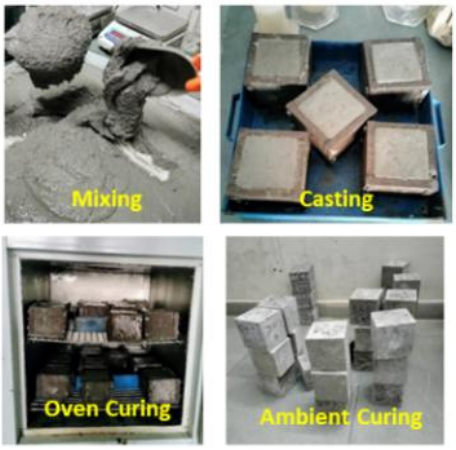


*Fig. 6 Production of GM*

(a) (b) (c)

*Fig. 7 Tests of the GM: (a) CS, (b) Fire Exposure, (c) Abrasion*

Initially, after 7 and 28 days of curing, CS of all GM was measured (Fig. 7(a)). Similar GM samples after 28 days of curing were placed in an electric furnace and exposed to extreme temperatures ranging from 500°C to 1000°C, starting at ambient temperature. The temperature in the furnace increased at a rate of 5°C/minute. When the furnace reached the desired temperature (500°C or 1000°C), the samples were heated for an additional 2 h (Fig. 7(b)). After 2 h of heating, the samples were cooled in an electric furnace for 24 h. Finally, the mass and CS of the GM specimens were measured again to compare with the earlier findings.

The GM underwent abrasion testing in accordance with IS 15658:2006 (Fig. 7(c)). The decrease in specimen volume after sixteen cycles was measured using Eq. 1. The thickness reduction was measured using a vernier caliper with a minimum count of 0.02 mm.

$$\Delta V = \frac{\Delta m}{PR} \quad (1)$$

Where,

ΔV (mm$^3$) = reduction in volume
Δm (g) = reduction in mass
PR = density of specimen in g/mm3

# 3. Results and Discussion

## 3.1 Effects of CPW On CS

Fig. 8 illustrates the 7-day CS of GM. The 7-day CS of GMV15 and GMW15 exceeded that of GPM across all curing regimes. Under ambient curing, the CS of GMV15 and GMW15 increased by 35.63% and 179% over GPM, respectively. The CS of the GMV15 and GMW15 cured at 60°C-24 h increased by 39.77% and 39.64%, respectively, relative to the GPM. Likewise, the CS of the above mixes cured at 60°C-48 h improved by 35.60% and 33.17%, respectively, in comparison to GPM.

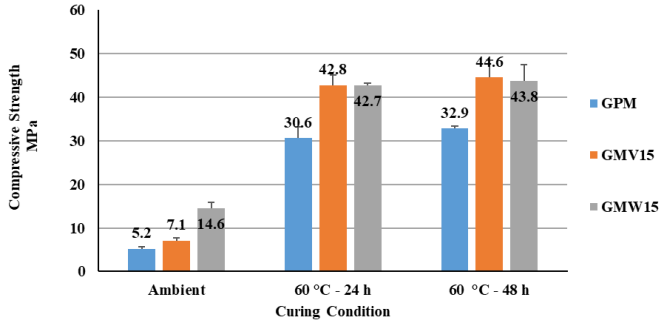


*Fig. 8 7-day CS of the GM*

Altering the oven curing duration from 24 h to 48 h has a negligible effect on the 7-day CS. The high-water absorption of CPW reduced the percentage of water in the mix, thereby improving the 7-day CS. The presence of lime in the WCPW boosted the CS (7 days) of GMW15 at ambient temperature and generated C-S-H and C-A-S-H gels (El-Dieb et al., 2018). The rate of geopolymerization for FA GPC is slow in ambient environments (Dissanayake, Dissanayake and Pathirana, 2022). At the

same time, heat curing accelerates the geopolymerization process and gives early CS (Hassan, Arif and Shariq, 2019). The curing conditions had a greater influence on the initial CS than the ultimate CS for low-calcium FA- and CWP-based geopolymer (Yılmaz, Degirmenci and Aygörmez, 2023). In this study, the use of CPW shows noticeable improvements in early-age CS (7 days) for all three curing methods. Another reason for the improvement of early CS was the increase of the Si/Al ratio as a replacement of FA by CWP (Mehmet Kaya, 2022).

Fig. 9 signifies the CS (28 days) of the GM. The CS of GPM and GMV15 was improved with a change in oven curing time (24 h to 48 h), but it was moderately decreased for GMW15 for 60°C-48 h.

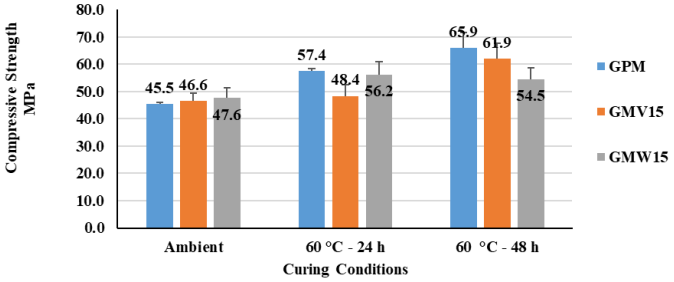


*Fig. 9 28-day CS of the GM*

At 28 days, the highest CS (65.9 MPa) was found for a GPM cured at 60°C-48 h. The lowest CS (45.46 MPa) was achieved in the GPM cured at ambient temperature. Minor improvement in 28-day CS was observed in GMV15 and GMW15 when ambient curing was adopted. This shows that CPW as FA replacement retains its final CS when ambient curing is adopted. On the contrary, the 28-day CS of GPM is higher in comparison to GMV15 and GMW15 for both oven curing systems. An increase in heat curing time improves the 28-day CS of all mixes (Tuyan, Andiç-Çakir and Ramyar, 2018). The extension of the curing period expedited the dissolution of the binder ingredients and enhanced geopolymerization. However, the lower silica content in the WCPW than in the VCPW (Table 1) may slow down the geopolymerization for 48 h of curing. $Fe_2O_3$ (Table 1) in FA increases CS for GPM as the oven curing time extends (Zailani et al., 2020).

## 3.2 Effect of heat exposure on GM

Prolonged exposure to high temperatures can substantially impact concrete's ability to withstand stresses. Fig. 10 illustrates how heat transmission alters the GM's colour. The colour of all samples remained unchanged after temperature exposure at 500°C. Eventually, it transformed to a brown shade upon heating to 1000°C. Spalling or cracks were not found on the surface of GM after temperature exposure. The alteration of brown colour because of heat exposure is attributed to the presence of high $Fe_2O_3$ content in FA (Sarker, Kelly and Yao, 2014; Zhang et al., 2020; Abd Razak et al., 2022).

### Effect on CS of GM due to heat exposure at 500°C

Fig. 11 presents the effects of heat exposure on CS for all the GM mixes. The residual CS (RCS) increased for GM made at 60°C-24 h. The improvement was noticed at 0.39%, 4.27%, and 3.04% for GPM, GMV15, and GMW15, respectively. Similar improvement in CS for FA GM cured at 60°C-24 h was reported in the past (Abd Razak et al., 2022). Also, all the GM cured at 60°C-24 h had RCS higher than 50 MPa, as shown in the orange line in Fig. 11. The increase in RCS is attributed to further geopolymerization because of heat treatment. This scenario shows the probable application of GM for heat-resistant precast products subject to moderate heat exposure up to 500°C.

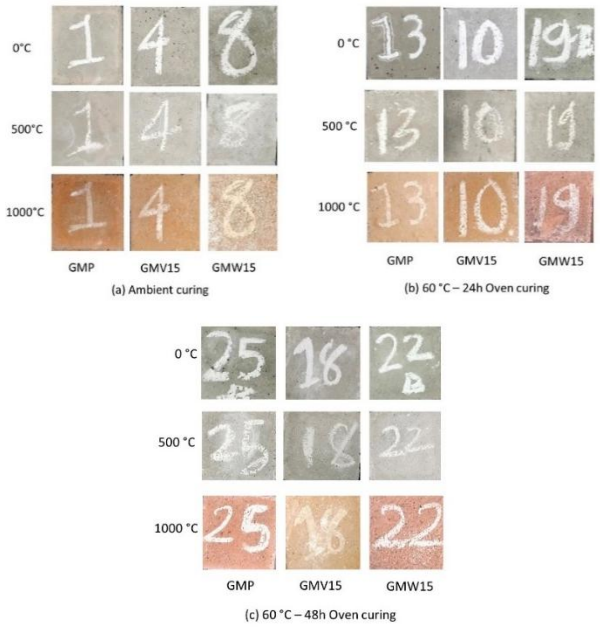


*Fig. 10 Mortar surface before and after temperature exposure*

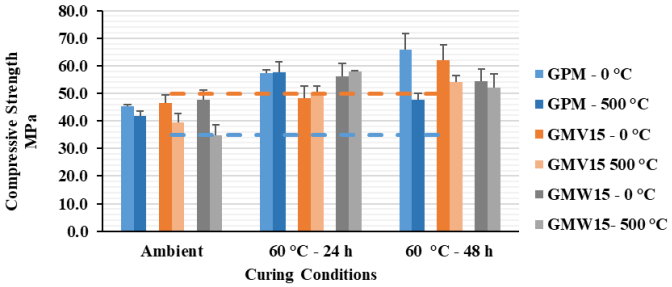


*Fig. 11 CS of GM before and after 500°C*

For ambient cured samples, 8.26%, 15.08%, and 26.84% reduction in CS was found in GPM, GMV15, and GMW15, respectively. Additionally, all ambient-cured GM maintained CS higher than 34 MPa, as shown by the blue line in Fig. 11. This finding indicates that even ambient-cured GM can be used for passive heat resistance for building and industrial applications.

At 60°C-48 h, the RCS of GPM was lower than that of GMV15 and GMW15. The reductions in CS due to exposure at 500°C were 27.68%, 12.67%, and 4.47% for GPM, GMV15, and GMW15, respectively. All mixes cured at 60°C-48 h exhibited RCS values exceeding 47 MPa. A comparable finding was previously documented, indicating that RCS was retained or augmented in air-cured samples subjected to heating at 800°C (Kaya et al., 2018). The compressive strength of geopolymer concrete increased following exposure to high heat as a result of the geopolymerization process (Davidovits, 1994). The results indicate that GMV15 and GMW15 cured at 60°C-24 h retained their RCS compared to those cured at 60°C-48 h and under ambient conditions. All mortars developed in this work demonstrated a higher CS (at 500°C) than those in the previous study (Table 4). The high molarity (14M) of mix and NS/NH ratio 2.5 gave the better resistant at 500°C exposure.

*Table 4. Comparison with literature for temperatures near 500°C*

| Authors | ID | Curing Time (days) | Curing conditions | NS / NH | NH Molarity | CS (MPa) | Temperature Exposure | RCS (MPa) |
|---|---|---|---|---|---|---|---|---|
| (Ezzedine El Dandachy *et al.*, 2024) | OPC<br>MK-based GM | 28 | Water<br>Ambient | -<br>2.5 | NA<br>16 M | 22<br>37.25 | 500°C-2 h | 3.53<br>35 |
| (Kaya *et al.*, 2018) | OPC<br>Fly ash GM | 28 | Water<br>50°C-48 h | - | NA<br>- | 37.98<br>36.13 | 600°C-1 h | 28.23<br>26.72 |
| (Yılmaz, Degirmenci and Aygörmez, 2023) | Fly ash GM | 28 | 60°C-24 h<br>60°C-48 h<br>60°C-72 h | 2<br>2<br>2 | 12 M<br>12 M<br>12 M | 38.62<br>38.83<br>51.22 | 600°C-2 h | 20.138<br>16.52<br>18.80 |
| Present study | GMW15 (Fly ash + WCPW) | 28 | Ambient<br>60°C-24 h<br>60°C-48 h | 2.5<br>2.5<br>2.5 | 14 M<br>14 M<br>14 M | 47.58<br>56.18<br>54.52 | 500°C-2 h | 34.81<br>57.89<br>52.08 |
| | GMV15 (Fly ash + VCPW) | 28 | Ambient<br>60°C-24 h<br>60°C-48 h | 2.5<br>2.5<br>2.5 | 14 M<br>14 M<br>14 M | 46.60<br>38.37<br>61.92 | 500°C-2 h | 39.46<br>50.47<br>54.08 |

### Effect on CS of GM due to heat exposure at 1000°C

The CS decreased for all samples following heat application at 1000°C. All GM mixes subjected to oven curing exhibited an RCS higher than 20 MPa (Fig. 12). The microcracks generated during oven curing exhibited further expansion upon exposure to 1000°C, resulting in a reduction of CS. The disintegration of C-A-S-H or N-A-S-H gels resulted in a reduction in the CS of GM (Rashad and Essa, 2020; Zhang et al., 2021).

Thermal stress and pressure within the pores interacted as a result of temperature gradients. In this scenario, the mortar is fractured due to the internal pressure surpassing its tensile strength (Yılmaz, Degirmenci and Aygörmez, 2023). The heat exposure led to the creation of dense geopolymer frameworks, which increase resistance and minimize thermal damage and disintegration. Room-cured GMs have a minor percentage loss in CS than temperature-cured GM (Fig. 12). The results can be validated with a previous study where specimens that were cured at 900°C had lower resistance to high temperatures, whereas specimens that were cured at comparatively moderate temperatures exhibited higher resistance (Yılmaz, Degirmenci and Aygörmez, 2023). For curing 60°C-24 h, GPM had less CS left over than GMV15 and GMW15. The result is in line with the GMV15 at 60°C-24 h (500°C exposure) performed best compared to other mixes. All mortars developed in this work demonstrated a higher CS (at 1000°C) than those in the previous study (Table 5).

The results show the possible application of ambient-cured GM for heat-resistant concrete where CS is required in the range of 15-20 MPa. The comparison also indicates that the 60°C-24 h is the optimum curing condition for heat resistance of low calcium materials, such as FA or CPW. Also, the NH molarity and NS/NH ratio affect the CS before and after heat exposure.

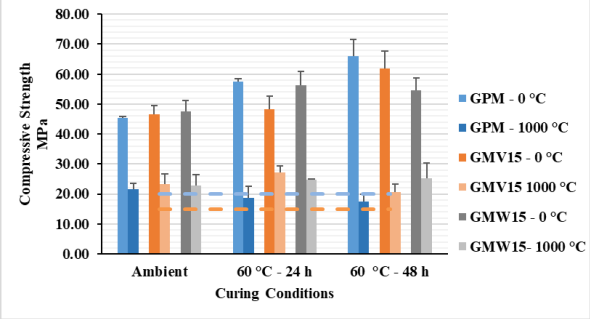


*Fig. 12 CS of GM before and after 1000°C*

### Temperature effects on mass loss

The mass reduction resulting from temperature exposure is typically associated with the evaporation of free water. The outcome is subject to heat application and its duration. Fig. 13 displays mass loss because of heat exposure. It ranged from 4.3% to 4.79% after 500°C exposure and 7.11% to 7.63% after 1000°C, respectively. As the temperature increased from 500°C to 1000°C, the mass loss increased. According to past research, normal and oven-cured GPCs have the same mass losses when subjected to extreme heat (Zhang et al., 2020). Mass losses of traditional concrete were found in the range of 5% - 8.75% for 500°C to 1200°C 2 h fire exposure (Abd Razak et al., 2022). Extreme heat has an immense effect on the mass loss of GM, although CPW replacement does not influence it.

## 3.3 Microstructure of GM

In the geopolymer, microstructural damage can occur due to dehydration, dihydroxylation, and thermal incompatibility between geopolymer paste and aggregates (Hassan et al., 2023). Fig. 14 displays the scanning electron microscopy (SEM) images of the GM after exposure at 1000°C. The microstructure consists of microcracks and micropores. A denser structure is visible, but the micropores appear within the gel matrix. The loss of bound water and deterioration of gel created porosity within the gel matrix. Similar kinds of microcracks and large micropores were reported at 800°C and 1000°C in the literature (Zhang et al., 2020).

The oven-cured samples are denser than the ambient-cured samples (Fig. 14). Also, the increasing temperature during time gives a dense microstructure after high-temperature exposure (Fig. 14 (d) to (i)). At the same time, larger microcracks are found in the samples cured at 48 h-60°C (Fig. 14 (g) to (i)). The development of microcracks caused the loss of CS. The GMV15 has smaller and fewer microcracks than GPM.

The use of CPW densifies the microstructure, but the effect is not visible at 1000°C. The larger microcracks were formed in GM mixes cured at 60°C-48 h. The heat curing creates microcracks during initial geopolymerization that expand further with extreme heat exposure.

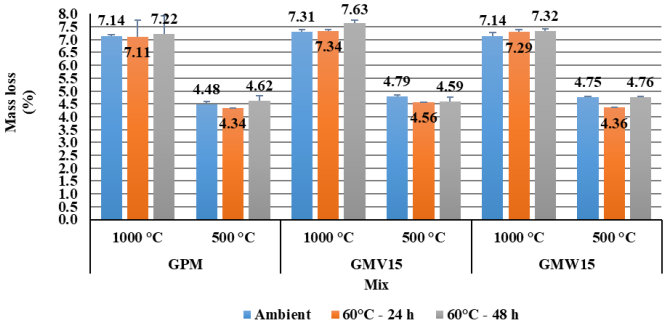


*Fig. 13 Mass loss after heat exposure*

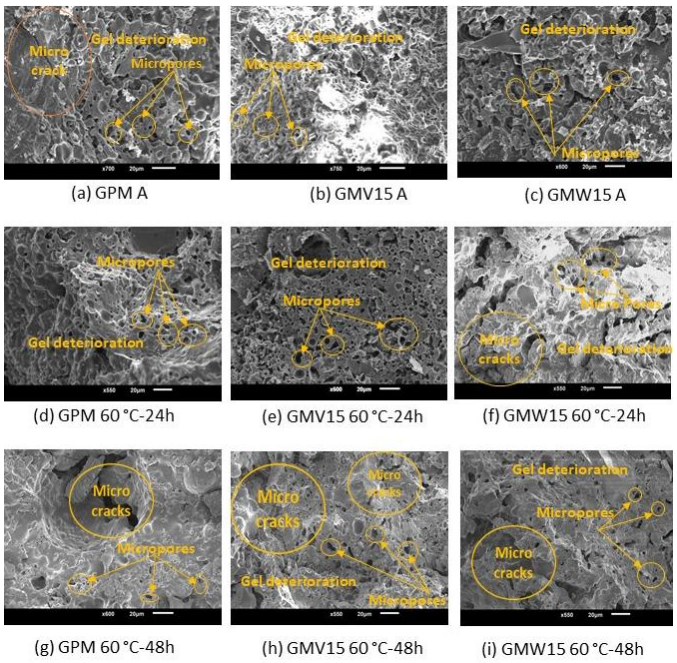


*Fig. 14 SEM of GM after 1000°C temperature exposure*

*Table 5. Comparison with literature for temperature near 1000°C*

| Authors | ID | Curing Time (days) | Curing conditions | NS / NH | NH Molarity | CS (MPa) | Temperature Exposure | RCS (MPa) |
|---|---|---|---|---|---|---|---|---|
| (Ezzedine El Dandachy *et al.*, 2024) | OPC | 28 | Water | - | NA | 21 | 900°C-2 h | 9 |
| | MK-based GM | | Ambient | 2.5 | 16 M | 38 | | 3 |
| (Kaya *et al.*, 2018) | OPC | 28 | Water | | NA | 38 | 800°C-1 h | 12 |
| | Fly ash GM | | 50°C-48 h | - | - | 7.63 | | 40.70 |
| (Yılmaz, Degirmenci and Aygörmez, 2023) | Fly ash GM | 28 | 60°C-24 h | 2 | 12 M | 38.2 | 900°C-2 h | 12 |
| | | | 60°C-48 h | 2 | 12 M | 38.2 | | 6 |
| | | | 60°C-72 h | 2 | 12 M | 51.5 | | 5.8 |
| Present study | GMW15 (Fly ash + WCPW) | 28 | Ambient | 2.5 | 14 M | 47.6 | 1000°C-2 h | 22.7 |
| | | | 60°C-24 h | 2.5 | 14 M | 56.18 | | 24.8 |
| | | | 60°C-48 h | 2.5 | 14 M | 54.5 | | 25.2 |
| | GMV15 (Fly ash + VCPW) | 28 | Ambient | 2.5 | 14 M | 46.6 | 1000°C-2 h | 23.4 |
| | | | 60°C-24 h | 2.5 | 14 M | 48.37 | | 27.4 |
| | | | 60°C-48 h | 2.5 | 14 M | 61.9 | | 20.7 |

The effect of temperature exposure on the microstructure of GMV15 cured at ambient conditions was shown on Fig. 15. An SEM image of a sample without fire exposure reveals geopolymer gel, voids, and unreacted FA particles.

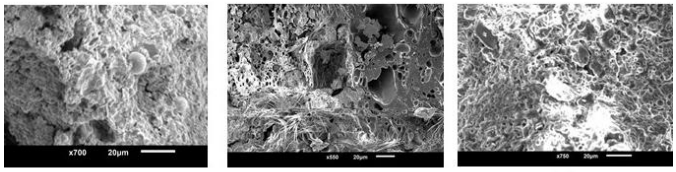

(a) 0 °C (b) 500 °C (c) 1000 °C

***Fig. 15 SEM of GMV15 A at different temperature exposures***

The structure of GMV15 after being heated to 500°C shows fibrous materials, suggesting that more geopolymerization happens because of the high temperature. Some microspores are also found at 500°C, which causes a reduction in CS. The development of geopolymer products at 500°C compensates for the loss of CS. The microstructure of GMV15 after 1000°C shows significant numbers of micropores and deterioration of the gel. The geopolymer product in GMV15 A at 500°C shows further polymerization. The loss in compressive strength (CS) due to the creation of micropores or microcracks is common when subjected to heat loss; however, the formation of geopolymer gel in GM at 500°C mitigated this CS loss. This is a different phenomenon compared to conventional mortar made by OPC.

### 3.4 Influence of Abrasion on GM

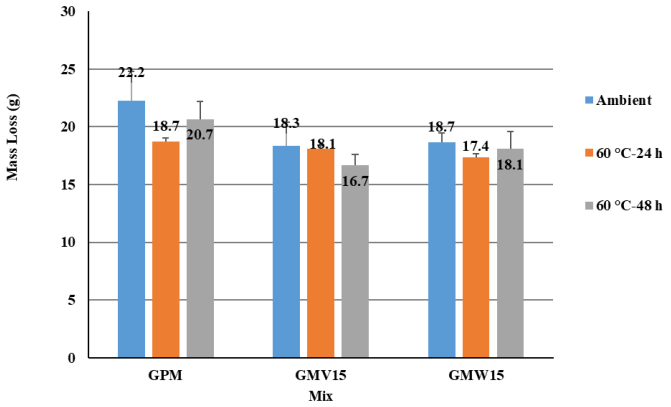


***Fig. 16 Reduction in mass under the abrasion test***

The abrasion wear of the GM is influenced by the paste strength and paste aggregate bond. Fig. 16 illustrates the decrease in mass after the abrasion test. For all curing methods, GPM exhibited greater mass loss than GMV15 and GMW15. The use of CPW improved the aggregate paste bonding. Past research reported similar behavior when crushed ceramic tile waste was used in place of fine aggregate (Abadel and Alghamdi, 2023).

The mean thickness reduction of GM is presented on Fig. 17. It is less than 1.5 mm for all samples. According to IS 15658:2006, the thickness loss should not exceed 6 mm. The use of CPW resist surface abrasion, hence GMV15 and GMW15, has lower thickness loss than GPM.

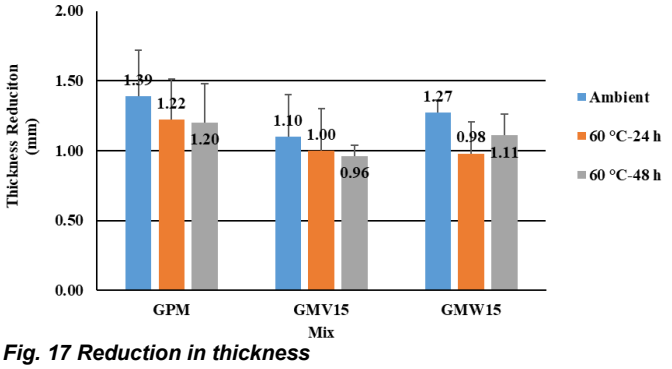


***Fig. 17 Reduction in thickness***

The abrasive wear for each mix per 1000 $mm^3$/5000 $mm^2$ was calculated (Fig. 18). The oven-cured samples demonstrated more improvement in abrasion resistance than the ambient-cured ones.

The replacement of FA with CPW improved the wear resistance of GM. Despite high 28-day CS, GPM showed higher abrasive wear than GMV15 and GMW15.

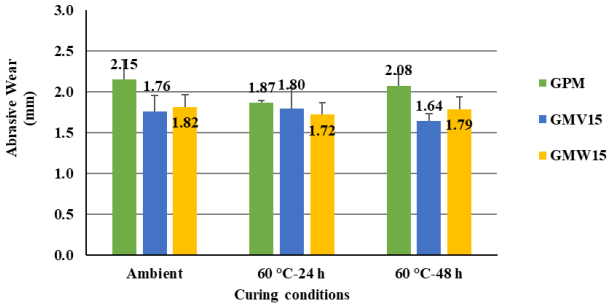


***Fig. 18 Abrasive wear***

## 4. Conclusions and Future Work

The work examined the impact of ceramic polishing waste (CPWs) and various curing processes on the initial and ultimate CS. Furthermore, the impact of high temperature exposure and abrasion on GM was investigated using modified blends. The use of CPW and variations in curing conditions significantly altered GM's physical and mechanical characteristics. The study presents the main results as follows: The conclusions highlight the effects of CPW and curing methods.

1) The CPWs influence the early-age CS; replacing VCPW and WCPW with FA improves the 7-day CS for ambience and temperature curing (24 h and 48 h). At the same time, temperature curing has a high impact on improving early-age CS for all GM mixes. The 28-day CS of the GM prepared with VCPW and WCPW was less than that of the FA-only mix for temperature curing, but it improved marginally when ambient curing was adopted. The combined effects of curing conditions and binder proportions can influence the final CS.
2) For 500°C-2 h exposure, GM made with FA and CPWs cured at 60°C-24 h or 48 h retained CS up to 47 to 50 MPa, while ambient cured samples can resist CS up to 34 MPa. Also, 60°C-24 h cured samples showed improvement in CS, where mixes with VCPW and WCPW have higher CS than the FA only mix.
3) At 1000°C-2 h heat exposure, the CS of all GM decreased. The mix of CPW improved the performance at this stage with higher RCS than the FA-only mix. The GM with CPW can resist CS up to 20 MPa.
4) GMV15 cured at 60°C-24 h performed best compared to other mixes subjected to heat exposure at 500°C and 1000°C.
5) Effects of CPW and curing conditions on mass loss of GM are negligible for heat exposure at 500°C and 1000°C.
6) The SEM analysis shows improvement in microstructure and further geopolymerization when heated at 500°C, but deterioration of gel particles and a greater number of micropores were formed at 1000°C, which reduces the CS.
7) The partial substitution of FA with 15% of VCPW and WCPW improved the abrasion resistance of GM. This effect is significant for ambient curing and 60°C-24 h oven curing.

The future scope of the study is to examine the heating and cooling impacts of CPW and fly ash-based GM. Additionally, the long-term durability effects can be evaluated for GM's corrosion resistance.

## Acknowledgment

The authors are thankful to Charotar University of Science and Technology for providing testing facilities to carry out the research work.

## Conflicts of interest

The authors have no conflicts of interest to declare.

## References

Abadel, A.A. and Alghamdi, H. (2023) 'Effect of high-volume tile ceramic wastes on resistance of geopolymer mortars to abrasion and freezing-thawing cycles: Experimental and deep learning modelling', Ceramics International, 49(10), pp. 15065–15081. Available at: https://doi.org/10.1016/j.ceramint.2023.01.089.

Abd Razak, S.N. et al. (2022) 'Fire performance of fly-ash-based geopolymer concrete: Effect of burning temperature on mechanical and microstructural properties', Materials Today: Proceedings, 66, pp. 2665–2669. Available at: https://doi.org/10.1016/j.matpr.2022.06.491.

Ahmed, J.K., Atmaca, N. and Khoshnaw, G.J. (2024) Exploring flexural performance and abrasion resistance in recycled brick-based engineered geopolymer composites', Beni-Suef University Journal of Basic and Applied Sciences, 13(1). Available at: https://doi.org/10.1186/s43088-024-00532-7.

Al-Hashem, M.N. et al. (2022) Mechanical and Durability Evaluation of Metakaolin as Cement Replacement Material in Concrete', Materials, 15(22). Available at: https://doi.org/10.3390/ma15227868.

Aly, S.T. et al. (2018) Properties of Ceramic Waste Powder-Based Geopolymer Concrete', International Congress on Polymers in Concrete (ICPIC 2018). Edited by M.M.R. Taha, pp. 429–435. Available at: https://doi.org/10.1007/978-3-319-78175-4_54.

Belaïd, F. (2022) 'How does concrete and cement industry transformation contribute to mitigating climate change challenges?', Resources, Conservation & Recycling Advances, 15, p. 200084.

Bhavsar, J.K. and Panchal, V. (2022) 'Ceramic Waste Powder as a Partial Substitute of Fly Ash for Geopolymer Concrete Cured at Ambient Temperature', Civil Engineering Journal (Iran), 8(7), pp. 1369–1387. Available at: https://doi.org/10.28991/CEJ-2022-08-07-05.

Bingöl, Ş. et al. (2020) 'Durability Properties of Geopolymer Mortars Containing Slag', Iranian Journal of Science and Technology - Transactions of Civil Engineering, 44(0123456789), pp. 561–569. Available at: https://doi.org/10.1007/s40996-019-00337-0.

Chindaprasirt, P. et al. (2010) 'High-strength geopolymer using fine high-calcium fly ash', Journal of Materials in Civil Engineering, 23(3), pp. 264–270.

Davidovits, J. (1994) 'Properties of geopolymer cements', in First international conference on alkaline cements and concretes, pp. 131–149.

Degirmenci, F.N. (2018) 'Freeze-Thaw and fire resistance of geopolymer mortar based on natural and waste pozzolans', Ceramics - Silikaty, 62(1), pp. 41–49. Available at: https://doi.org/10.13168/cs.2017.0043.

Dissanayake, D.M.H., Dissanayake, D.M.A.K. and Pathirana, C.K. (2022) 'Strength properties of Fly Ash based Geopolymer Concrete cured at different temperatures', Electronic Journal of Structural Engineering, 22(2), pp. 19–26. Available at: https://doi.org/10.56748/ejse.223262.

El-Dieb, A.S. et al. (2018) 'Ceramic waste powder: from landfill to sustainable concretes', Proceedings of the Institution of Civil Engineers - Construction Materials, 171(3), pp. 109–116. Available at: https://doi.org/10.1680/jcoma.17.00019.

Ezzedine El Dandachy, M. et al. (2024) Effect of Elevated Temperatures on Compressive Strength, Ultrasonic Pulse Velocity, and Transfer Properties of Metakaolin-Based Geopolymer Mortars, 14(7), p. 2126. Available at: https://doi.org/10.3390/buildings14072126.

Hager, I., Sitarz, M. and Mróz, K. (2021) 'Fly-ash based geopolymer mortar for high-temperature application – Effect of slag addition', Journal of Cleaner Production, 316. Available at: https://doi.org/10.1016/j.jclepro.2021.128168.

Hassan, A. et al. (2023) 'Fire resistance characteristics of geopolymer concrete for environmental sustainability: a review of thermal, mechanical and microstructure properties', Environment, Development and Sustainability, 25(9), pp. 8975–9010. Available at: https://doi.org/10.1007/s10668-022-02495-0.

Hassan, A., Arif, M. and Shariq, M. (2019) 'Effect of curing condition on the mechanical properties of fly ash-based geopolymer concrete', SN Applied Sciences, 1(12), pp. 1–9. Available at: https://doi.org/10.1007/s42452-019-1774-8.

Herbudiman, B. et al. (2024) 'Effect of Different Ceramic Waste Powder on Characteristics of Fly Ash-Based Geopolymer', Civil Engineering Journal (Iran), 10(02), pp. 431–443. Available at: http://dxdoi.org/10.28991/CEJ-2024-010-02-06.

Huseien, G.F. et al. (2018) 'Waste ceramic powder incorporated alkali activated mortars exposed to elevated Temperatures: Performance evaluation', Construction and Building Materials, 187, pp. 307–317. Available at: https://doi.org/10.1016/j.conbuildmat.2018.07.226.

IS 15658 (2006) Indian Standard Precast Concrete Blocks for Paving - Specification. Bureau of Indian Standards.

IS 383:2016 (2016) 'Indian Standard Specification for Coarse and Fine Aggregates from Natural Sources for Concrete, Bureau of Indian Standards, New Delhi.

Joshi, S. V. and Kadu, M.S. (2012) 'Role of Alkaline Activator in Development of Eco-friendly Fly Ash Based Geo Polymer Concrete', International Journal of Environmental Science and Development, (January 2012), pp. 417–421. Available at: https://doi.org/10.7763/ijesd.2012.v3.258.

Kalinowska-Wichrowska, K. et al. (2024) Properties of Geopolymer Mixtures Incorporating Recycled Ceramic Fines', Materials, 17(8). Available at: https://doi.org/10.3390/ma17081740.

Kaya, M. et al. (2018) 'Behaviour of geopolymer mortars after exposure to elevated temperatures', Medziagotyra, 24(4), pp. 428–436. Available at: https://doi.org/10.5755/j01.ms.24.4.18829.

Kaya, M (2022) 'Magazine of Civil Engineering Mechanical properties of ceramic powder based geopolymer mortars', 112(11207), pp. 20–22. Available at: https://doi.org/10.34910/MCE.112.7.

Kaya, Mehmet (2022) 'The effect of micro-SiO2 and micro-Al2O3 additive on the strength properties of ceramic powder-based geopolymer pastes', Journal of Material Cycles and Waste Management, 24(1), pp. 333–350. Available at: https://doi.org/10.1007/s10163-021-01323-3.

Krishna Rao, A. and Kumar, D.R. (2020) 'Effect of various alkaline binder ratio on geopolymer concrete under ambient curing condition', Materials Today: Proceedings, 27, pp. 1768–1773. Available at: https://doi.org/https://doi.org/10.1016/j.matpr.2020.03.682.

Memiş, S. and Bılal, M.A.M. (2022) 'Taguchi optimization of geopolymer concrete produced with rice husk ash and ceramic dust', Environmental Science and Pollution Research, 29(11), pp. 15876–15895. Available at: https://doi.org/10.1007/s11356-021-16869-w.

Nayana, A.M. and Rakesh, P. (2018) 'Strength and durability study on cement mortar with ceramic waste and micro-silica', Materials Today: Proceedings, 5(11, Part 3), pp. 24780–24791. Available at: https://doi.org/https://doi.org/10.1016/j.matpr.2018.10.276.

Negahban, E., Bagheri, A. and Sanjayan, J. (2023) 'Investigation of abrasion resistance of geopolymer concrete cured in ambient temperature for pavement applications', Road Materials and Pavement Design, 24(11), pp. 2641–2662. Available at: https://doi.org/10.1080/14680629.2022.2161934.

Patel, H., Arora, N.K. and Vaniya, S.R. (2015) 'Use of ceramic waste powder in cement concrete', International Journal for Innovative Research in Science & Technology, 2(1), pp. 91–97.

Phul, A.A. et al. (2019) 'GGBS And Fly Ash Effects on Compressive Strength by Partial Replacement of Cement Concrete', Civil Engineering Journal (Iran), 5(4), pp. 913–921. Available at: https://doi.org/10.28991/cej-2019-03091299.

Ramujee, K. and Potharaju, M. (2014) 'Permeability and abrasion resistance of geopolymer concrete', Indian Concrete Journal, 88(12), pp. 34–43.

Rashad, A.M. and Essa, G.M.F. (2020) 'Effect of ceramic waste powder on alkali-activated slag pastes cured in hot weather after exposure to elevated temperature.', Cement and Concrete Composites, 111, p. 103617. Available at: https://doi.org/10.1016/j.cemconcomp.2020.103617.

Raval, A.D., Patel, D.I.N. and Pitroda, J. (2013) 'Ceramic waste: Effective replacement of cement for establishing sustainable concrete', International Journal of Engineering Trends and Technology (IJETT), 4(6), pp. 2324–2329.

Runganga, D., Okonta, F. and Musonda, I. (2024) 'Strength and Durability Properties of High-Volume Fly Ash (HVFA) Binders: A Systematic Review', CivilEng, 5(2), pp. 435–460. Available at: https://doi.org/10.3390/civileng5020022.

Saranya, P., Nagarajan, P. and Shashikala, A.P. (2019) 'Development of Ground-Granulated Blast-Furnace Slag-Dolomite Geopolymer Concrete', ACI Materials Journal, 116(6), pp. 235–243. Available at: https://doi.org/10.14359/51716981.

Sarker, P.K., Kelly, S. and Yao, Z. (2014) 'Effect of fire exposure on cracking, spalling and residual strength of fly ash geopolymer concrete', Materials and Design, 63, pp. 584–592. Available at: https://doi.org/10.1016/j.matdes.2014.06.059.

Saxena, R. and Gupta, T. (2022) 'Assessment of mechanical, durability and microstructural properties of geopolymer concrete containing ceramic tile waste', Journal of Material Cycles and Waste Management, 24(2), pp. 725–742. Available at: https://doi.org/10.1007/s10163-022-01353-5.

Singh, N.B. (2018) Fly ash-based geopolymer binder: A future construction material', Minerals, 8(7). Available at: https://doi.org/10.3390/min8070299.

Tuyan, M., Andiç-Çakir, Ö. and Ramyar, K. (2018) 'Effect of alkali activator concentration and curing condition on strength and microstructure of waste clay brick powder-based geopolymer', Composites Part B: Engineering, 135, pp. 242–252. Available at: https://doi.org/https://doi.org/10.1016/j.compositesb.2017.10.013.

Vilas Meena, R. et al. (2022) '"Impact of waste ceramic tile on resistance to fire and abrasion of self-compacting concrete"', Materials Today: Proceedings, 60, pp. 167–172. Available at: https://doi.org/https://doi.org/10.1016/j.matpr.2021.12.287.

Witzke, F.B. et al. (2023) 'Abrasion resistance of metakaolin-based geopolymers through accelerated testing and natural wear', Wear, 530–531, p. 204996. Available at: https://doi.org/https://doi.org/10.1016/j.wear.2023.204996.

Wong, L.S. (2022) Durability Performance of Geopolymer Concrete: A Review', Polymers, 14(5). Available at: https://doi.org/10.3390/polym14050868.

Yanti, E.D. et al. (2024) Utilization of various ceramic waste as fine aggregate replacement into fly ash-based geopolymer', Materials Letters, 357, p. 135651. Available at: https://doi.org/https://doi.org/10.1016/j.matlet.2023.135651.

Yılmaz, A., Degirmenci, F.N. and Aygörmez, Y. (2023) 'Effect of initial curing conditions on the durability performance of low-calcium fly ash-based geopolymer mortars', Boletin de la Sociedad Espanola de Ceramica y Vidrio [Preprint]. Available at: https://doi.org/10.1016/j.bsecv.2023.10.006.

Zailani, W.W.A. et al. (2020) Effect of Iron Oxide ($Fe_2O_3$) on the Properties of Fly Ash Based Geopolymer', IOP Conference Series: Materials Science and Engineering, 877(1). Available at: https://doi.org/10.1088/1757-899X/877/1/012017.

Zareei, S.A. et al. (2017) 'Rice husk ash as a partial replacement of cement in high strength concrete containing micro silica: Evaluating durability and mechanical properties', Case Studies in Construction Materials, 7(October 2016), pp. 73–81. Available at: https://doi.org/10.1016/j.cscm.2017.05.001.

Zhang, G.Y. et al. (2021) 'Effect of waste ceramic powder on the properties of alkali–activated slag and fly ash pastes exposed to high temperature', Polymers, 13(21). Available at: https://doi.org/10.3390/polym13213797.

Zhang, H. et al. (2020) Deterioration of ambient-cured and heat-cured fly ash geopolymer concrete by high temperature exposure and prediction of its residual compressive strength', Construction and Building Materials, 262, p. 120924. Available at: https://doi.org/10.1016/j.conbuildmat.2020.120924.

## Disclaimer